FRPRCS-6, Singapore, 8–10 July 2003
Edited by Kiang Hwee Tan

OPTIMAL COST DESIGN FOR BEAMS PRESTRESSED WITH FRP TENDONS

I. BALAFAS and C. J. BURGOYNE
University of Cambridge, Department of Engineering
Trumpington Street, Cambridge, CB2 1PZ, UK

While most of the technical questions concerning structural integrity of concrete structures prestressed with fibre reinforced plastic bars have already been solved, their application is limited to prototype structures due to their high initial cost. The paper proposes a method for selecting structural dimensions that are optimised with respect to cost. By observing the sensitivity of the optimum solution to various factors, more efficient ways to use those materials in structures can be found.

INTRODUCTION

Research on the application of fibre-reinforced plastics (FRPs) in concrete structures has been extensive. FRPs are a suitable alternative reinforcing material but their high initial cost hinders their use, partly due to the high cost of prototype batches. The high cost means little demand, so there is little incentive for the composites industry to invest in the civil engineering market. This paper arises from a study to investigate the various cost interactions in the market for FRP reinforced or prestressed structures[1].

One of the drawbacks in design with FRPs is their brittle nature. Plastic behaviour gives warning of failure, and in indeterminate structures, moment redistribution can occur. In prestressed concrete (PSC) structures with FRP tendons, plastic deformations can come from concrete when properly confined[2]. Recent work on FRP prestressed beams confined in the compression zone with aramid spirals showed extensive non-linear characteristics in the load deflection curve[3]. By adjusting the bond conditions between concrete and reinforcement, the desired concrete crushing failure mode can be achieved[4].

FRPs only give high stresses at high strains, which is considered problematic in reinforced concrete design, but this can create advantageous conditions when used in PSC structures. The high strength of the bars can be utilised by pre-straining[5], at the same time reducing the problem of excessive deflections at the service load. The low stiffness can also be

beneficial by minimising the losses that result from creep and shrinkage of the concrete.

In this study, determinate PSC beams are analysed and the design constraints identified. The depth of the section and the area of reinforcement are taken as the primary design parameters, and when all the design constraints are taken into account, a feasible zone is created on a plot of depth versus bar area. By introducing a costing function to the problem the most economic structures can be found, and a parametric study can reveal how design parameters affect cost. Alsayed & Al-Salloum[6] used a similar approach when optimising concrete structures reinforced with FRPs.

DESIGN CONSTRAINTS: ULTIMATE CONDITIONS

Sectional analysis

The structure is assumed to be a simply-supported beam loaded with a uniformly distributed ultimate load of $w=1.4G+1.6LL$, where G and LL are the service dead- and live-loads respectively.

A sectional analysis is carried at midspan, using standard well-known assumptions. Initially, it is necessary to assume a position for the tendon (and hence its eccentricity). It will be assumed to be as low as practicable in the section in order to maximise the moment capacity, but this is adjusted later if working load stress conditions are critical.

The strain is assumed to vary linearly through the depth of the beam, and allowance is made for partial or fully unbonded structures; incremental tendon strains are multiplied by a bond reduction coefficient Ω_u[7]. For single point loading with unbonded tendons, $\Omega_u=1.5/(l/d_{ps})$, and for three point or uniform loading $\Omega_u=3.0/(l/d_{ps})$, where l is the span and d_{ps} the static depth. Equivalent values do not yet exist for partially bonded tendons, so for the current work a parametric study was performed.

Material law

Concrete can be confined or unconfined. Passive FRP spiral reinforcement can be used to confine the concrete in compression. The model developed by Leung[3] is used to draw the stress-strain properties of both plain and passively confined concrete, taking data from actively confined concrete tests (Figure 1). In this study a simpler triaxial model is used[8]. The failure strain for plain concrete is taken as 0.0035 and for passively confined concrete occurs at snapping of the spiral, when the concrete's lateral expansion is more than the spiral's failure strain.

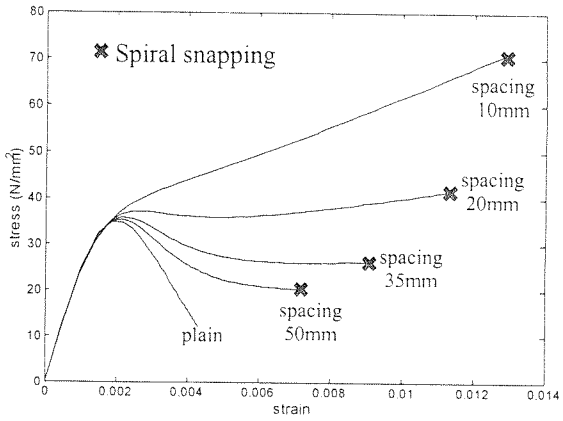

Figure 1. Concrete stress-strain curves (aramid spiral 2.5mm diameter)

FRPs are linear elastic up to failure. Steel is linear elastic up to yielding and strain hardens up to snapping, with a slope of $(f_u-f_y)/(e_u-e_y)$, where (e_u, f_u), (e_y, f_y) are strain and stress values at the maximum load and yielding load respectively.

Moment capacity

Two modes of failure can occur at the ultimate load: crushing of concrete or tendon snapping. In the first case the concrete strain at the top fibre is fixed at the concrete failure strain (confined or unconfined as appropriate). By assuming a tendon area, the force and moment equilibrium equations can be solved for the beam depth and bottom fibre strain (ε_b, Figure 2). If the resulting tendon strain is greater than the snapping strain of the bar, the bar strains are fixed as the bar snapping strain and the system is solved for top strain (ε_t) and section depth. The systems to be solved are non-linear but can be solved for a range of bar areas using Newton-Raphson. The results represent beams with the same strength, but different material proportions. Figure 3 shows typical results of such an analysis on a plot of required section depth against reinforcement. The line marked "ultimate" represents a lower bound on combinations of section dimensions, which have adequate capacity at the ultimate load.

Limiting reinforcement ratios

If it is assumed that tendon snapping is undesirable with FRP tendons, a minimum reinforcement ratio (ρ_{min}) can be determined which represents beams with balanced concrete crushing and reinforcement snapping modes

of failure. This can also be plotted as shown on Figure 3. Similarly, for beams prestressed with steel tendons, where over-reinforcement is deemed to be unacceptable, a maximum reinforcement ratio (ρ_{max}) can be found.

DESIGN CONSTRAINTS: WORKING CONDITIONS

At the working load, the structure must satisfy deflection and allowable stress conditions with partial safety factors for load set to unity. The beam can be either cracked or uncracked, depending on the prestressing class, but otherwise the materials are assumed to be linearly elastic.

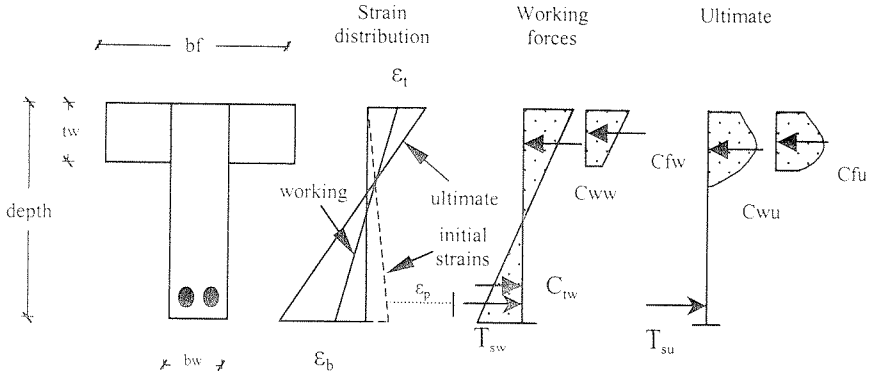

Figure 2. Working and ultimate sectional analysis at midspan section

A sectional analysis is performed using (for unbonded and partially bonded beams) the strain reduction factors Ω for uncracked and cracked elastic PSC sections[9].

Deflections

Deflections can be found by integrating twice the curvatures, along the span. For a simply supported beam uniformly loaded without variations in the cross section or reinforcement ratio across span, the deflections can be given in the closed form $\Delta=(10/96)\psi_m l$, where l is span and ψ_m the average curvature. If cracks are permitted at service conditions then the CEB formula[10] can be used[11] to interpolate cracked and uncracked curvatures:

$$\psi_m = \zeta\psi_1 + (1-\zeta)\psi_2 \qquad (1)$$

where ψ_1, ψ_2 are the curvatures for state 1 (uncracked) and state 2 (cracked) respectively, and ζ is the CEB interpolating coefficient.

Creep effects are taken into account using an age adjusted effective modulus, which allows for external loads developing gradually with time. Shrinkage can be considered in the calculations as a compressive strain induced at the centroidal level. Equilibrium redistributes those strains in the section.

The compatibility and equilibrium equations can then be used to determine the three unknown parameters: the top and bottom strains (ε_t, ε_b) and the depth of the beam. They can be found by solving the three equations for force & moment equilibrium and deflection. The solutions represent structures, which deflect equally for the given moment. Such a solution is shown on Figure 3 as the "deflection" line. This also represents a lower bound and in this particular case is a more severe constraint than the ultimate load condition.

Allowable stress constraints

For determinate PSC structures, the four stress constraints that govern are: (a) tension and compression at transfer, (b) tension and compression at the maximum service load. These apply for both top and bottom fibres, but if the beam is assumed to be in sagging bending, then it is known which four of these conditions apply. For an uncracked section the elastic equation for each stress limit can be solved for section depth while varying the tendon area. A modified approach is needed if the section is cracked. This process results in a further four bound lines on Figure 3. Two will be upper bounds; two will be lower bounds.

DEPTH-TENDON AREA DIAGRAM

Figure 3 now shows all the constraints from the design process. Cracking could also have been included but this example is fully prestressed. The result is a feasible zone, which shows acceptable combinations of tendon area and section depth. The transfer stress bounds the zone from the right, the minimum tendon area limits from the top and one (or a combination) of the limits imposed by ultimate, deflection or working stress conditions governs from the bottom left. In the case illustrated by the figure, the tensile stress limit at the working load defines the bottom left part of the feasible zone.

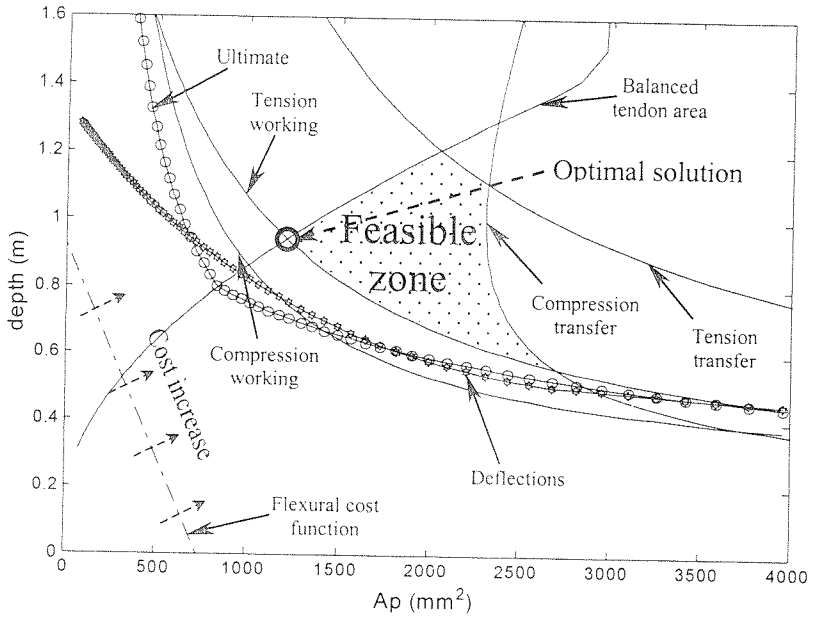

Figure 3. Typical depth - tendon area diagram, aramid partially bonded beam.

The flexural cost function is also shown on the figure, which takes into account the expense of concrete, tendon, confining reinforcement and formwork. Lines of equal cost take the form of parallel lines, one of which is shown as a chain-dashed line in the bottom left of Figure 3. One of the most important effects of changing from steel to FRP is that the slope of this line alters. The cost function moves with the same slope towards greater depths and tendon areas as the cost increases. The optimum flexural solution occurs where the increasing costing function line meets the feasible zone. In the example shown in Figure 3 this is clearly where the working tension and minimum tendon area constraints coincide.

TENDON ECCENTRICITY

At the beginning of the analysis a tendon eccentricity was assumed. If the section is governed by the ultimate load condition, a reasonable assumption is that the most cost-effective section is one with the tendon as near the bottom fibre of the section as possible. But this may not be allowed if the transfer stress constraints are so strict that they eliminate the feasible zone entirely. In such cases the analysis is repeated with lower eccentricity. The

transfer stress constraints move to the right and a feasible zone is formed as in Figure 3. The eccentricity for which a feasible zone just forms is the optimum. Figure 4 shows three possible Magnel diagrams. Figure 4a shows the normal case where the maximum tendon eccentricity is valid. Figure 4b shows the case where the tension constraint at transfer would be violated at the maximum tendon eccentricity, which forces a new optimal solution. The section also has to be large enough to allow the existence of a feasible zone on the Magnel diagram. In the present analysis this can be forced by adjusting the relative depth of the tendon. This results in a Magnel diagram as in Figure 4c.

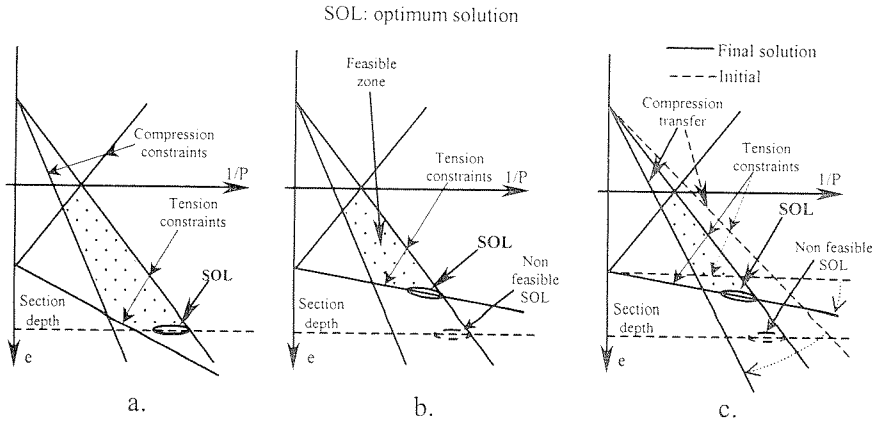

Figure 4. Magnel diagrams at optimum feasible and non feasible sections.

SHEAR

To allow for shear forces, shear reinforcement is provided following recent modifications on the normal 45^0 truss analogy which is used for shear predictions on beams with steel reinforcement[12]. Full details are to be found elsewhere[1]. The principal addition to the method given above is to allow for the cost of the shear stirrups; this may alter the slope of the cost function on Figure 3, and thus may alter the optimal solution, but it does not affect the other constraints on the design.

EXAMPLE

The principles given above were applied to a typical simply supported beam structure with a straight-profile prestressing tendon. The beam had a clear span of 13m and a cross section as shown in Figure 2. The web is 0.25m wide and the flange is 0.15m thick and 5m wide with an effective width of 1.05m wide. The beam is loaded with its own weight and a 2 kN/m^2 live load. The beam is prestressed with steel, aramid (Fibra or Parafil rope) or carbon (CFRP) tendons. Their properties are shown in Table 1.

Table 1: Tendon properties

	Steel	AFRP (Fibra)	Parafil rope (Kevlar 49)	CFRP
Strength (MPa)	1752	1480	1964	2200
Elastic Modulus (GPa)	210	68.6	112	130
Failure Strain	0.1	0.02	0.017	0.013
Cost (Euros/m^3)	5930	27010	27010	28860

Concrete strength was taken as 50 MPa and the partial material safety factors were 1.5 for concrete, 1.05 for steel and 1.3 for all FRPs. The creep factor was taken as 3 and a shrinkage strain of 0.0003. The stress limits were: transfer tension 1 MPa, transfer compression 18 MPa, working tension 0 MPa and working compression 25 MPa. The concrete cost in Euros/m^3 for the southern parts of UK follows the formula: $C_{concrete}=54.4e^{0.006fc}$ where f_c is in MPa[13]. Beam stirrups, in this example, had the same material as their tendons. For steel tendons, low strength (460 MPa) steel was used for stirrups, with cost 4420 Euros/m^3.

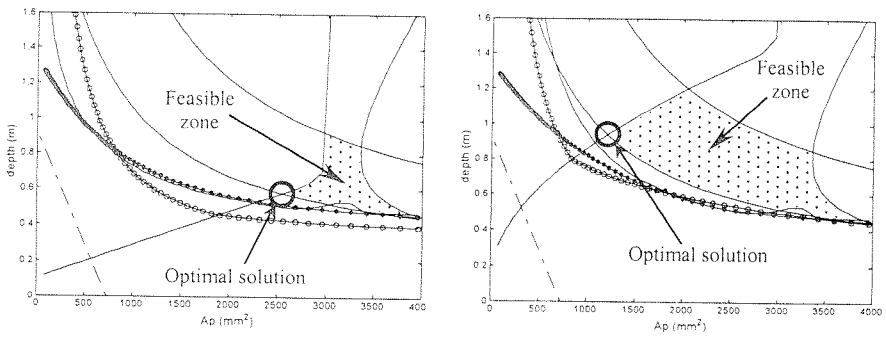

a. Fully bonded b. Unbonded

Figure 5. Typical depth versus tendon areas diagrams

The beams were prestressed in different ways: from fully bonded to fully unbonded with plain or confined compression concrete. The optimal cost solution for each form of construction can be found in Table 2. Figure 5 shows typical plots of tendon area versus section depth for two extreme cases: fully bonded and fully unbonded CFRP tendons are shown.

It is found that in the case of steel PSC cost is virtually constant because in all optimum cases the steel yields. The small cost difference is due to effects of slight strain hardening, and thus higher stress and lower steel area when the tendon is bonded.

In contrast, for beams prestressed with FRPs, the lowest cost comes from fully unbonded beams. The optimal solution for a bonded beam tends to be shallower with a larger tendon (Figure 5a), but for the unbonded beam the optimum is deeper with a smaller tendon (Figure 5b).

The presence of spirals in the compression zones adds cost to the final solution, but in most cases they should be provided because concrete can fail in a brittle and catastrophic manner. The additional costs can be justified from the improved structural characteristics of such structures. By providing confinement concrete, fails gently, thus the structure can give warning and show non-linear characteristics before failure.

Table 2. Cost (Euros) simply supported beams prestressed with steel and FRPs

	Bonded	unbonded	partial bonded 1	partial bonded 2	partial bonded (spiral spacing 60 mm)	partial bonded (spiral spacing 30 mm)	unbonded (spiral spacing 60 mm)	unbonded (spiral spacing 30 mm)
Steel	439.3	441.1	440.7	440.3				
Fibra	1539.6	945.2	963.5	1151.8	1504.8	1908.9	1200.5	1549.6
Parafil		833.8					1184.2	1533.7
Carbon	1238.8	886.9	946.5	1076.5	1425.1	1845.7	1186.1	1538.1

CONCLUSIONS

The method described above allows the optimal determination of the parameters of concrete structures prestressed with fibre reinforced plastic tendons. The feasible zone that results when the design constraints are plotted on a depth versus tendon area diagram allows the observation of the behaviour and interactions of the various parameters on the final solutions. As a result lessons can be learnt on how best to use the properties of expensive FRP. In particular, beams prestressed with FRP should be unbonded.

ACKNOWLEDGEMENT

The authors wish to acknowledge the European Commission for funding the EU TMR Network "ConFibreCrete".

REFERENCES

1. Balafas, I. (2003). *Economic Viability of FRP concrete Structures*, PhD Thesis, Cambridge University, in preparation.
2. Kotsovos, M.D. and Pavlovic, M.N. (1995), *Structural Concrete*, Thomas Telford Publications, 512 pp.
3. Leung, H. Y. (2000), *Study of Concrete Confined with Aramid Spirals*, PhD Thesis, Cambridge.
4. Lees J.M. (1997). *Flexure of Concrete Beams Pre-Tensioned with Aramid FRPs*, PhD thesis, Department of Engineering, University of Cambridge, UK.
5. Burgoyne, C. J. (1993). *Should FRPs be Bonded to Concrete?*, SP-138, Nanni & Dolan (eds.), American Concrete Institute: 367-380.
6. Alsayed, S.H. and Al-Salloum, Y.A. (1996). *Optimisation of Flexure Environment of Concrete Beams Reinforced with Fibre-Reinforced Plastic Bars*, Magazine of Concrete Research, 48(174): 27-36.
7. Naaman, A.E. and Alkhairi, F.M. (1991). *Stress at Ultimate Post-Tensioning Tendons: Part 2 – Proposed Methodology*, ACI Structural Journal, 88(6): 683-692.
8. Ahmad, S.H. and Shah, S.P. (1982). *Complete Triaxial Stress-Strain Curves for Concrete*, ASCE, 108(ST4): 728-742.
9. Naaman, A.E. (1990). *A New Methodology for the Analysis of Beams Prestressed with External or Unbonded Tendons*, External Prestressing in Bridges", ACI Special Publication SP-120, American Concrete Institute, 1990: 339-354.
10. Beeby A.W., Favre R., Koprna M. and Jaccoud J.P. (1985). *Cracking and Deformations*, CEB design manual, Lausanne.
11. Eurocrete (2000). *Design Recommendations of FRP Reinforced Concrete Structures*, First Draft, Riga, Latvia.
12. Guadagnini, M. Pilakoutas, K. and Waldron, P. (1999). *Shear Design for Fibre Reinforced Polymer Reinforced Concrete Elements*, SP-138, Dolan et al (eds.), American Concrete Institute, Michigan, Selected Presentations Proceedings: 11-21.
13. Ablemix (2002), Private communication.